

RAPID *IN VIVO* ADC MAPPING OF HYPERPOLARIZED ^{13}C METABOLITES ON A CLINICAL 3T MR SCANNER

Bertram L. Koelsch^{1,2}, Galen D. Reed^{1,2}, Kayvan R. Keshari³, Robert A. Bok¹, Daniel B. Vigneron^{1,2}, John Kurhanewicz^{1,2}, and Peder E. Z. Larson^{1,2}

¹Department of Radiology and Biomedical Imaging, UCSF, San Francisco, CA, United States, ²UC Berkeley - UCSF Graduate Program in Bioengineering, San Francisco, CA, United States, ³Memorial Sloan-Kettering Cancer Center, NY, United States

Introduction: Apparent diffusion coefficient (ADC) maps of water have become useful for prostate cancer identification and characterization.¹ Differences in local water mobility create contrast in these images, which in turn give an indication of the local tissue microstructure. The growing field of hyperpolarized ^{13}C has also proven to be useful in identifying tumors by measuring the real-time metabolism of hyperpolarized ^{13}C pyruvate to lactate.² Yet, while *in vivo* MRSI and MRI studies spatially localize these hyperpolarized ^{13}C metabolites, they do not give an indication of their distribution within the local tissue microstructure based on their mobility. Understanding this distribution could help elucidate what fraction of hyperpolarized ^{13}C lactate signal is vascular versus within dense tumor tissue. Aggressive tumors, for example, have been shown to transport higher fractions of lactate into the extracellular environment.³ Recent work has laid the foundation for hyperpolarized ^{13}C diffusion-weighted MR^{4,6} and showed improved tumor contrast with diffusion weighting.⁷ In this study, we developed a novel diffusion-weighted hyperpolarized ^{13}C EPI sequence on a clinical 3T MR scanner to rapidly obtain ADC maps of hyperpolarized ^{13}C metabolites *in vivo*.

Experimental Methods: All experiments used a 3T clinical MRI scanner (GE) equipped with 4 G/cm peak gradient amplitude (1.5 G/cm/ms peak slew rate) and a dual-tuned mouse birdcage coil. Hyperpolarized ^{13}C diffusion experiments were performed using a pulsed gradient double spin echo sequence with a single-shot flyback echo planar imaging (EPI) readout (Fig 1); $T_E=175\text{ms}$, $T_R=250\text{ms}$, $\text{FOV}=4\times 8\text{cm}$ (3.3x3.3mm resolution). To efficiently use the entire non-renewable hyperpolarized magnetization, spectral spatial excitation pulses with a specified progressive flip angle scheme (Fig 1) provided constant signal in the absence of diffusion gradients. A pair of adiabatic sech/tanh pulses⁸ produced the spin echo. Diffusion gradient pairs surrounding the refocusing pulses were given opposite polarity to generate large ^{13}C diffusion b-values, even with clinical gradient strength constraints.

A HyperSense (Oxford Instruments) was used to polarize ^{13}C pyruvate. Upon dissolution, the hyperpolarized sample was either injected into a 60mL phantom or into a transgenic mouse with prostate cancer (TRAMP). Each hyperpolarized ^{13}C metabolite was imaged 4 times within 1s, thus minimizing signal changes due to T_1 or metabolism. After a flip angle correction based on a simultaneously acquired double-angle transmit B_1 map (see below), ADC maps were generated by fitting the diffusion weighted images on a per-voxel basis according to $\text{ADC} = -\ln(S/S_0) / b$.

Results and Discussion: To validate the sequence, we imaged hyperpolarized ^{13}C pyruvate in room temperature phantoms (n=3) (Fig 2). Considering that the progressive flip angle scheme repeatedly samples the non-renewable hyperpolarized signal, flip angle errors propagate through all acquisitions. Our simulations showed that for the experimental parameters used here, flip angle errors of 20% could cause 20% errors in the ADCs. To correct for this source of error and increase the quantitative robustness of the ADC measurements, we generated a hyperpolarized ^{13}C metabolite specific B_1 map. Calculated by comparing the last 2 images with the double angle identity $\sin(2\theta) = 2\sin(\theta)\cos(\theta)$ and accounting for the non-renewable signal, the B_1 map was used for voxel-wise flip angle corrections across all images. The ADC map for hyperpolarized ^{13}C pyruvate, showing a mean $\text{ADC} = 1.09 \times 10^{-3} \text{mm}^2/\text{s} \pm 0.20 \times 10^{-3}$, corresponds with previous solution measurements.⁴

Hyperpolarized ^{13}C pyruvate and lactate were imaged in TRAMP mice bearing prostate tumors (n=3) (Fig 3). The image overlay of hyperpolarized ^{13}C lactate with minimal diffusion weighting (Fig 3b, left) shows lactate signal throughout the abdominal area. The same acquisition with a high degree of diffusion weighting (Fig 3b, right) shows only hyperpolarized ^{13}C lactate from the tumor, thereby increasing tumor contrast. The ADC map shows lower ADCs in the tumor ($\text{ADC} = 0.35 \times 10^{-3} \text{mm}^2/\text{s} \pm 0.09$) than those found higher in the abdomen ($\text{ADC} = 0.6-1.8 \times 10^{-3} \text{mm}^2/\text{s}$ depending on location). Further studies will use hyperpolarized ^{13}C lactate ADC maps to improve tumor localization and pathologic grading in prostate cancer.

Conclusion: This study is the first demonstration of ADC mapping of hyperpolarized ^{13}C metabolites on a clinical 3T MR scanner. The pulsed gradient double spin echo EPI sequence allows us to rapidly acquire diffusion-weighted images and generate ADC maps at clinically translatable SNR and spatial resolution. This is possible despite both gradient amplitude limitations and the lower MR sensitivity of ^{13}C . Clinically, ADC mapping of hyperpolarized ^{13}C lactate could allow for improved classification of tumor grade and metastatic potential by measuring both enhanced metabolic flux and differences in lactate's microenvironment.

Acknowledgements: Support from the U.S. National Institute of Health grants R00-EB012064, P41-EB013598 and R01-CA166655.

References: [1] Nagarajan *et al. Advances in Urology* **2012**, 1–5 (2012). [2] Albers *et al. Cancer Research* **68**, 8607 (2008). [3] Ganapathy *et al. Pharmacol Therapeut* **121**, 29–40 (2009). [4] Koelsch *et al. Analyst* **138**, 1011 (2013). [5] Schilling *et al. NMR in Biomedicine* **26**, 557–568 (2013). [6] Kettunen *et al. Magn. Reson. Med.* **70**, 1200–1209 (2013). [7] Larson *et al. IEEE Trans Med Imaging* **31**, 265–275 (2012). [8] Cunningham *et al. J Magn Reson* **187**, 357–362 (2007).

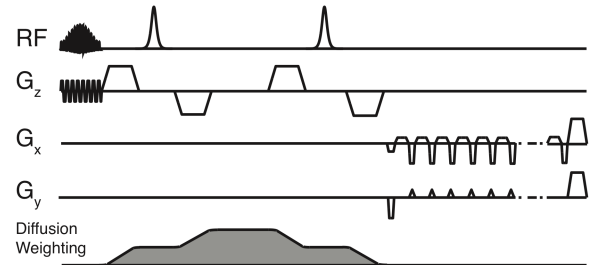


Figure 1. The pulsed gradient double spin echo sequence with an echo-planar imaging readout. The table shows the experimental parameters used for each hyperpolarized ^{13}C metabolite acquisition.

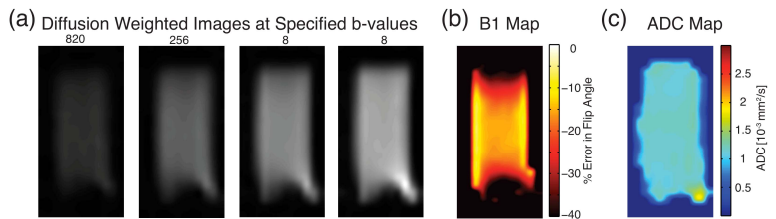


Figure 2. Phantom studies with hyperpolarized ^{13}C pyruvate. (a) The diffusion weighted EPI images of hyperpolarized ^{13}C pyruvate taken at the various b-values. (b) The transmit B_1 map created from the difference in signal between the last 2 diffusion-weighted images and the double-angle identity (see text). (c) The ADC map of hyperpolarized ^{13}C pyruvate in solution.

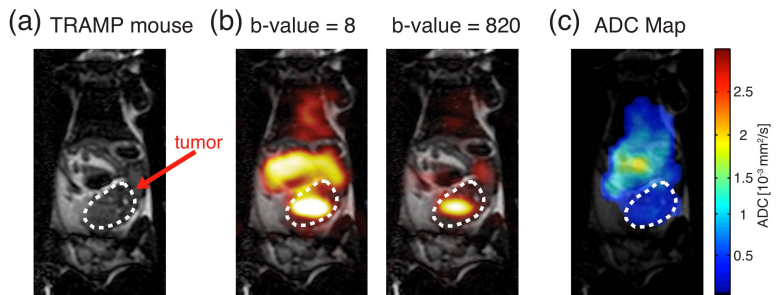


Figure 3. ADC mapping of hyperpolarized ^{13}C lactate in a TRAMP mouse. (a) A fast spin echo proton image with the arrow pointing at the tumor. (b) Low and high b-value overlay EPI images of hyperpolarized ^{13}C lactate. (c) The ADC map of hyperpolarized ^{13}C lactate.